Probing protein–protein interactions in real time

Mario B. Viani, Lia I. Pietrasanta, James B. Thompson, Ami Chand, Ilse C. Gebeshuber, Johannes H. Kindt, Michael Richter, Helen G. Hansma and Paul K. Hansma

Department of Physics, University of California at Santa Barbara, Santa Barbara, California 93106, USA.

We have used a prototype small cantilever atomic force microscope to observe, in real time, the interactions between individual protein molecules. In particular, we have observed individual molecules of the chaperonin protein GroES binding to and then dissociating from individual GroEL proteins, which were immobilized on a mica support. This work suggests that the small cantilever atomic force microscope is a useful tool for studying protein dynamics at the single molecule level.

The atomic force microscope (AFM) has proven to be a useful tool for studying proteins at the single molecule level. In particular, the AFM has been used to measure both structural[1–3] and mechanical properties[4–6] of individual proteins in physiologically relevant buffers. The AFM has also been used, to a lesser extent, to observe the activity of individual proteins by detecting protein motion[7,8]. These studies have been restricted, in part, by both the noise and speed limitations of the AFM. Recently, however, it has been shown that small cantilever AFMs can be used for making faster and quieter measurements[9]. In this work, we used a small cantilever AFM[10] to observe individual protein interactions. We have observed, in real time, individual *Escherichia coli* GroES proteins binding to and then subsequently dissociating from individual *E. coli* GroEL proteins. This work suggests that the small cantilever AFM is a useful tool for studying protein dynamics at the single molecule level.

The *E. coli* chaperonin GroEL and its co-chaperonin GroES play important roles in helping proteins reach their native states. GroEL and GroES work together in a series of ATP-mediated steps to capture misfolded proteins, free them from local energy minima, and finally provide them with an environment conducive to folding to their native states[11–14]. Both X-ray crystallography[15–18] and cryoelectron microscopy[19,20] studies have been used to resolve the structures of GroEL and the GroEL–GroES complex in different stages of the folding cycle. The time dependence of the folding cycle has been probed in bulk samples by experiments that employ hydrogen exchange[21], fluorescence techniques[22–25], and surface plasmon resonance[26].

The surface plasmon resonance studies[26] demonstrate that GroEL proteins adsorbed onto a support still retain their ability to bind and release GroES. This observation led us to believe that it would be possible to observe the interaction between GroEL and GroES with an AFM. Previous AFM studies of the chaperonin system by Mou *et al.*[1,2] used contact mode (in which the tip scans the sample at constant force) to obtain high resolution static images of both GroEL and GroES adsorbed to mica in solution. In these studies, the authors state that it was often difficult to image the proteins more than once, unless they had been treated with a fixative such as glutaraldehyde. This is consistent with our experiences with commercial AFMs. In our study reported here, we used a prototype AFM[10] designed to work with small cantilevers (Fig. 1*a*), which can image both GroEL and the GroEL–GroES complex in solution repeatedly without the aid of fixing agents. This led us to try to observe the association and dissociation of individual GroEL–GroES complexes.

Imaging GroEL and GroEL–GroES

A small cantilever AFM image of a monolayer of GroEL molecules in buffer solution is shown in Fig. 1*b*. The central channel of the protein ring can be resolved on many of the molecules, which is consistent with previous AFM observations that GroEL adsorbs to mica in an end-up orientation[1]. The average diameter of the molecules in this image is 14.6 ± 2.2 nm, which agrees well with both X-ray[15] and cryoelectron microscopy[19] data. Upon the addition of GroES and ADP into the buffer solution, GroES molecules were observed as features that extend ~3 nm higher than the GroEL film (Fig. 2). The height of these features is also consistent with X-ray crystallography[15–18] and cryoelectron microscopy[19] data. We were able to repeatedly scan the same sample region without excessively disturbing the GroEL–GroES complexes. This is demonstrated in Fig. 2, which shows the first and last of seven consecutive scans of the same sample region. Most of the GroES proteins remain attached to the GroEL film at the same location throughout the scanning. To verify that the interactions between GroES and GroEL were specific, we also tried adding GroES to the buffer without ADP. In this case, we did not observe any GroES molecules binding to the GroEL film, which is consistent with solution experiments that have shown that GroEL and GroES do not interact in the absence of nucleotides.

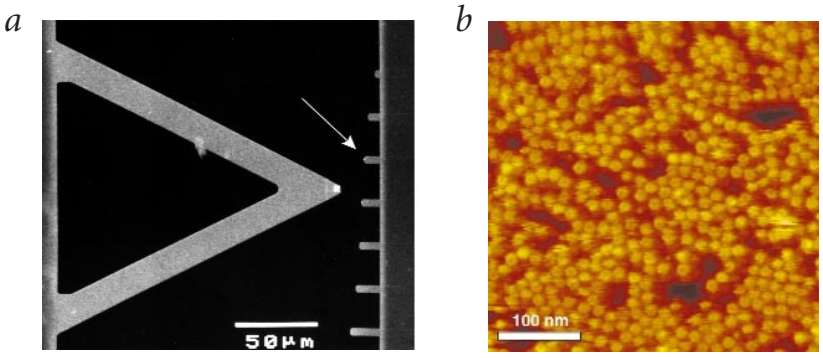

Fig. 1 Small cantilevers and image of GroEL taken with the small cantilever AFM. ***a***, This scanning electron micrograph shows an array of prototype small cantilevers (on the right) next to a commercially available cantilever. Compared to commercially available cantilevers, for a given spring constant, small cantilevers yield higher resonant frequencies, thereby allowing faster measurements. They also are able to detect smaller forces than larger cantilevers[9]. The results reported here were obtained using cantilevers similar to the one indicated by the arrow. This cantilever has approximately the same spring constant as the commercial cantilever and a resonant frequency 30 times greater. Our prototype microscope[10] can use small cantilevers because it focuses the laser beam onto the cantilever with a spot diameter of ~3 µm (compared to ~20 µm in commercial microscopes). ***b***, This height image of GroEL adsorbed on mica in buffer solution (full height scale, from black to yellow, is 15 nm) was taken by running our small cantilever AFM in tapping mode. The central channels of the GroEL molecules are visible as a dark region at the center of a bright ring. These fields of densely packed molecules could be imaged repeatedly with small cantilevers. The image (256 × 256 pixels) was taken with a scan rate of 10.2 Hz.

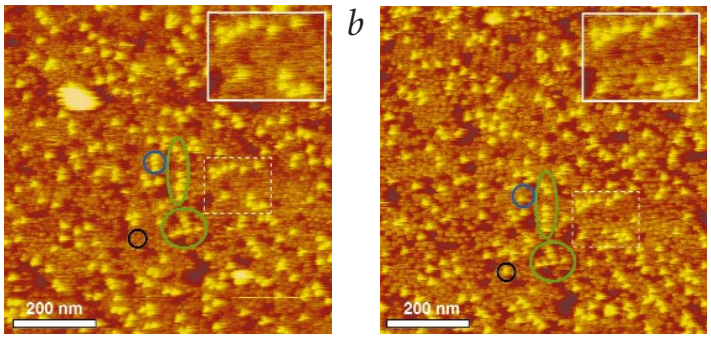

Fig. 2 GroEL and isolated GroEL–GroES complexes in buffer solution on a mica support. ***a***,***b*** The first and last images, respectively, of seven consecutive images of a film of GroEL with isolated GroEL–GroES complexes. The GroES can be seen as the bright (that is, tall) features that extend above the level of the GroEL film. The GroEL–GroES complexes are ~3 nm taller than the surrounding film. Note that most of the GroES proteins remained attached to the film in the same location. For example, the green ellipses identify two groups of molecules that are present in both images. The black circle identifies a molecule that has attached at some time after the original image was captured. The blue circle highlights three molecules in which two become unbound before the final image. The insets (upper right corner of each image) provide enlarged views of the sample region inside the (dashed) box.The final concentrations of GroES and ADP in the buffer solution were 100 nM and 0.2 mM.

Although small cantilever AFMs are able to scan biological samples such as DNA much faster than conventional AFMs[10], we found that we were unable to scan the GroEL–GroES complex (which is much more fragile than DNA) with tip speeds much faster than 20 μm s^{-1} due to the limited bandwidth of the feedback electronics. Therefore, in order to obtain the temporal resolution required for observing the formation and dissociation of the GroEL–GroES complexes in the presence of Mg-ATP, we scanned the sample in one dimension rather than two. By repeatedly scanning a single line across the sample we were able to monitor the height of a series of protein molecules at rates as high as 20 Hz. This method[8] is illustrated in Fig. 3, which shows an image of GroEL molecules in buffer in which the slow scan axis was disabled half way through the scan. From this image it is clear that each 'tube' is associated with a single protein molecule. The height variations along the length of the tubes reflect the time dependent changes in the protein structure.

GroEL–GroES complex formation and dissociation

The images of the tubes shown in Figs 3 and 4*a* were taken in a buffer solution that did not contain Mg-ATP or GroES. Under these conditions we typically observed root mean square height variations of ~0.5 nm (Fig. 4*b*). However, upon the addition of both GroES and Mg-ATP, we observed that many of the tubes displayed repetitive well-defined step-like variations in height (Fig. 4*c*). The cross section of the two featured tubes clearly shows the step-like variations in height (Fig. 4*d*). The magnitude of these steps is 3.6 ± 1 nm. This is consistent with the height difference measured between structures of GroEL and the GroEL–GroES complex obtained by X-ray crystallography[15–18] and cryoelectron microscopy[19] studies. We therefore conclude that the observed height variations are caused by a GroES molecule attaching to and then separating from the GroEL molecule associated with the tube. It is important to emphasize that we observed these step-like variations in height only when the buffer solution contained both GroES and Mg-ATP. This implies that the height fluctuations we observed in the presence of Mg-ATP and GroES are caused by complex formation and not by nonspecific interactions between GroEL and GroES, or by Mg-ATP activated motion of the GroEL.

In repeated experiments, we identified multiple tubes in which we saw two or more cycles of complex formation and dissociation. In one case, we recorded an active molecule for ~2 min and saw the complex form and dissociate 18 times. A histogram of the complex lifetime for this molecule is shown in Fig. 5. The distribution of complex lifetime is peaked near 5 s and the average lifetime is ~7 ± 1 s (n = 18). This distribution is representative of all active molecules that we observed.

Control experiment

To quantify the effect that tip–sample interactions were having on the measured complex lifetimes, we performed the following control experiment. First GroE complex lifetimes were measured in the presence of ADP alone (0.2 mM). After acquiring data for ~30 min, Mg-ATP was added to the buffer (making the concentrations of Mg-ATP and ADP 2.5 mM and 0.14 mM, respectively) and the complex lifetimes were re-measured. After adding the Mg-ATP to the buffer, the lifetime of the complex had a distribution similar to what is shown in Fig. 5. However, in the presence of ADP alone, the complex lifetime was much longer. In fact, a majority of the ADP complexes did not dissociate at all within the time of observation. (Our current observation time was limited by thermal drift of the microscope and was usually on the order of one minute.) From bulk measurements, the half-life of the complex in the presence of ADP has been shown to be ~4 h[26]. We observed, however, that a small percentage (< 10%) of complexes had lifetimes < 30 s. We hypothesize that this small percentage of events may reflect the effects of tip–sample interactions. We cannot, however, rule out the possibility of short complex lifetimes, in the presence of ADP, for some of the molecules based on our data alone.

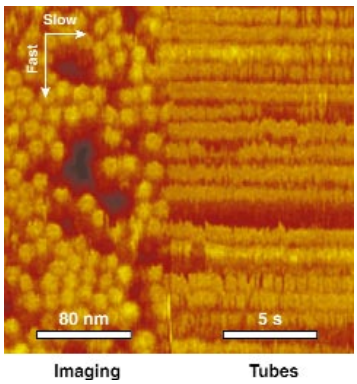

Fig. 3 GroEL scanned in two dimensions (left) and in one dimension (right). In this image of GroEL, the slow scan axis was disabled half way through the scan. After the slow scan axis was disabled, the tip repeatedly scanned the same line of proteins, thereby generating protein 'tubes'. Each tube corresponds to an individual protein molecule. The advantage of recording tubes is that it is possible to monitor the heights of molecules at much higher temporal resolution (100 ms here) than allowable with conventional imaging in two dimensions (25 s here) because the rest of the field does not need to be imaged before returning to the molecules of interest. The long and short arrows indicate the directions of the fast and slow scan axes respectively.

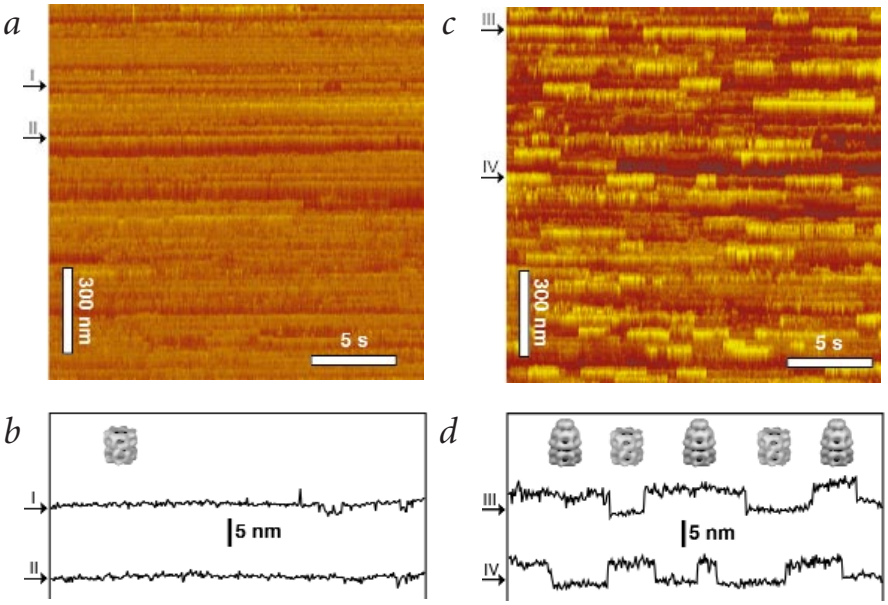

Fig. 4 Association and dissociation of the GroEL–GroES complex. ***a***, These tubes of GroEL were scanned at 15.3 Hz in buffer solution that did not contain GroES. ***b***, The cross sections of two selected tubes show typical height fluctuations. The first cross section shows some structure towards the right end of the trace that is probably caused by the protein being pushed around by the tip. ***c***, After the addition of GroES (144 nM) and Mg-ATP (2.5 mM) into the buffer solution, we observed large repeated variations in height along the lengths of many tubes. ***d***, The cross sections of these tubes show the height stepping between two values that differed by 3.6 ± 1 nm. This height variation is consistent with the height differences seen between GroEL and the GroEL–GroES complex in cryoelectron microscopy and X-ray crystallographic data. Therefore, we conclude that we are observing the association and dissociation of the complex at the single molecule level. This is depicted with the aid of cryoelectron microscopy images of GroEL and the GroEL–GroES complex reported by Roseman *et al.*[20].

Immobilized GroEL is a model system

The GroE system studied here is a model system that differs from solution experiments because the GroEL is adsorbed onto a support, thereby making one of the GroEL rings inaccessible to GroES. However, pioneering work on this type of model system has established its relevance. Burston *et al.*[27] showed that a modified mixed-ring GroEL protein, in which one of the rings was unable to bind GroES or substrate polypeptides, showed kinetics for the refolding of rhodanese that were identical to those of the wild type GroEL. It is not essential, therefore, for both rings of GroEL to be accessible to GroES in order for the protein to retain its normal activity. This conclusion is also supported by Hayer-Hartl *et al.*[26], who showed through surface plasma resonance experiments that the immobilization of the GroEL proteins on a support did not destroy their functional properties.

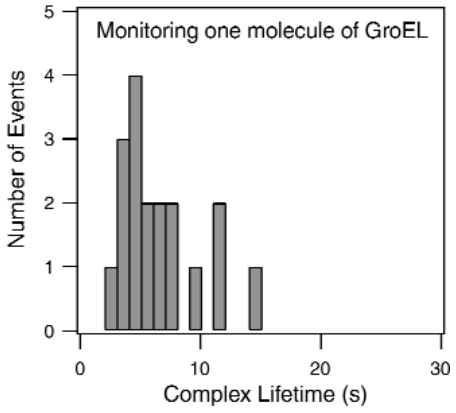

Fig. 5 Measured complex lifetime of an individual GroEL molecule in the presence of Mg-ATP and GroES. We observed individual GroES molecules attach to and then separate from the same GroEL molecule 18 times over an observation time of ~2 min. This histogram shows the distribution of complex lifetimes that we measured during the observation time. Note the absence of events with lifetimes < 2 s. As pointed out by Lu *et al.*[34], a non-exponential distribution can be expected when there are one or more intermediate steps in a process, even when all individual steps are exponential.

Comparison to bulk experiments

The distribution of the lifetimes of the complex is peaked near 5 s, which is significantly shorter than lifetimes determined from bulk measurements (15–30 s; refs 25,26,28). The difference in measured lifetimes may be caused by differences in the experimental conditions, such as the immobilization of GroEL. However, we also note that comparing results of the bulk experiments to results of these single molecule experiments is problematic. For example, many of the bulk experiments measured lifetimes for an ensemble of proteins with an unknown distribution of initial states, whereas these experiments measured lifetimes of single molecules with a well-defined initial state. Another problem is that bulk experiments and single molecule experiments do not measure the same functional form for the distribution of complex lifetimes: the bulk experiments measure an exponential distribution while these single molecule experiments measure a non-exponential distribution.

Finally, we note that the distribution of complex lifetimes we measured agrees well with the distribution measured in the only other single molecule study of the GroE system of which we are currently aware. Taguchi *et al.*[29] reported a non-exponential distribution for the complex lifetimes peaked at 5 s, which they measured using a single molecule fluorescence technique. This is significant because the distribution that Taguchi *et al.* measured is similar to the distribution that we measured (Fig. 5), despite completely different experimental techniques (optical fluorescence *versus* AFM) and different orientations of the GroEL molecules (sideways *versus* end-up) on different supports (glass *versus* mica).

Our experiments demonstrate the possibility of using the small cantilever AFM as a tool for studying the dynamics of single proteins. This technique will augment other single molecule methods that use optical techniques, by allowing real time measurements of length changes associated with protein activity.

Methods

Imaging. All imaging was performed in a prototype AFM designed to be used with small cantilevers[9,10,30–32]. The prototype AFM detects the motion of small cantilevers by using high numerical aperture

optics to focus a laser beam onto the cantilever and then measuring angular changes in the reflected light beam. The cantilevers (Fig. 1) were fabricated out of low stress silicon nitride using standard micromachining techniques[9]. The cantilevers used were typically 10 μm long, 5 μm wide, and 75 nm thick. Each cantilever had an electron beam deposited tip that was 1–2 μm long. The spring constants were approximately 60–120 pN nm^{-1} and the resonant frequencies in water were 130–200 kHz. All imaging was done in tapping mode[33] to minimize sample damage. The tapping frequency was usually chosen to be 130 kHz and the free amplitude of oscillation was set to 10–20 nm. All imaging was performed at ambient temperature.

Sample preparation. GroEL was purified from overexpression in *E. coli* (SIGMA) and reconstituted to 1 mg ml^{-1} (50 mM Tris, 150 mM KCl, 10 mM $MgCl_2$, 1 mM dithiothreitol (DTT) and 2.5% (w/v) trehalose, pH 7.5). The samples were prepared for imaging by applying a 10 μL drop of GroEL solution to freshly cleaved mica. After incubation at room temperature for ~30 min, the sample was rinsed with buffer (50 mM HEPES (pH 7.5), 50 mM KCl and 10 mM $MgCl_2$) to remove loosely bound GroEL proteins, and then imaged in this same buffer. The GroES was purified from overexpression in *E. coli* (SIGMA) and reconstituted to 0.25 mg ml^{-1} (25 mM Tris, 75 mM KCl, 0.5 mM DTT and 1.25% (w/v) trehalose, pH 7.5) and diluted in buffer (50 mM HEPES (pH 7.5), 50 mM KCl and 10 mM $MgCl_2$).

Acknowledgments

We thank G. Lorimer for his encouragement and many useful suggestions. We thank H. Saibil for her generous permission to use the cryo-electron microscopy images of GroEL and the GroEL–GroES complex. The Materials Research Division and the Molecular Biophysics Division of the National Science Foundation supported this work.

Correspondence and requests for materials should be addressed to M.B.V. *email: viani@physics.ucsb.edu*

Received 24 May, 2000; accepted 23 June, 2000.

1. Mou, J., Sheng, S. J., Ho, R. & Shao, Z. *Biophys. J.* **71**, 2213–2221 (1996).
2. Mou, J., Czajkowsky, D.M., Sheng, S.J., Ho, R. & Shao, Z. *FEBS Lett.* **381**, 161–164 (1996).
3. Muller, D.J. & Engel, A. *J. Mol. Biol.* **285**, 1347–1351 (1999).
4. Rief, M., Gautel, M., Oesterhelt, F., Fernandez, J.M. & Gaub, H.E. *Science* **276**, 1109–1112 (1997).
5. Oberhauser, A.F., Marszalek, P.E., Carrion-Vazquez, M. & Fernandez, J.M. *Nature Struct. Biol.* **6**, 1025–1028 (1999).
6. Oesterhelt, F. *et al. Science* **288**, 143–146 (2000).
7. Radmacher, M., Fritz, M., Hansma, H.G. & Hansma, P.K. *Science* **265**, 1577–1579 (1994).
8. Thomson, N.H. *et al. Biophys. J.* **70**, 2421–2431 (1996).
9. Viani, M.B. *et al. J. Appl. Phys.* **86**, 2258–2262 (1999).
10. Viani, M.B. *et al. Rev. Sci. Instrum.* **70**, 4300–4303 (1999).
11. Hartl, F.-U. *Nature* **381**, 571–580 (1996).
12. Ranson, N.A., White, H.E. & Saibil, H.R. *Biochem. J.* **333**, 233–242 (1998).
13. Sigler, P.B. *et al. Annu. Rev. Biochem.* **67**, 581–608 (1998).
14. Fink, A.L. *Physiol. Rev.* **79**, 425–449 (1999).
15. Braig, K. *et al. Nature* **371**, 578–586 (1994).
16. Hunt, J.F., Weaver, A.J., Landry, S.J., Gierasch, L. & Eisenhofer, J. *Nature* **379**, 37–45 (1996).
17. Boisvert, D.C., Wang, J., Otiwonowski, Z., Horwich, A.L. & Sigler, P.B. *Nature Struct. Biol.* **3**, 170–177 (1996).
18. Xu, Z., Horwich, A.L. & Sigler, P.B. *Nature* **388**, 741–750 (1997).
19. Chen, A. *et al. Nature* **371**, 261–264 (1994).
20. Roseman, A.M., Chen, S., White, H., Braig, K. & Saibil, H.R. *Cell* **87**, 241–251 (1996).
21. Shtilerman, M., Lorimer, G.H. & Englander, S.W. *Science* **284**, 822–825 (1999).
22. Weissman, J.S. *et al. Cell* **83**, 577–587 (1995).
23. Sparrer, H., Lilie, H. & Buchner, J. *J. Mol. Biol.* **258**, 74–87 (1996).
24. Rye, H.S. *et al. Nature* **388**, 792–798 (1997).
25. Rye, H.S. *et al. Cell* **97**, 325–338 (1999).
26. Hayer-Hartl, M.K., Martin, J. & Hartl, F.-U. *Science* **269**, 836–841 (1995).
27. Burston, S.G., Weissman, J.S., Farr, G.W., Fenton, W.A. & Horwich, A.L. *Nature* **383**, 96–99 (1996).
28. Burston, S.G., Ranson, N.A. & Clarke, A.R. *J. Mol. Biol.* **249**, 138–152 (1995).
29. Taguchi, H., Tadakuma, H., Ueno, T., Yoshida, M. & Funatsu, T. *Biophys. J.* **78**, 36A (2000).
30. Walters, D.A. *et al. Rev. Sci. Instrum.* **67**, 3583–3590 (1996).
31. Schaffer, T.E. *et al. Proc. SPIE* **3009**, 48–52 (1997).
32. Walters, D.A. *et al. Proc. SPIE* **3009**, 43–47 (1997).
33. Hansma, P.K. *et al. Appl. Phys. Lett.* **64**, 1738–1740 (1994).
34. Lu, H. P., Xun, L. & Xie, X. S. *Science* **282**, 1877–1881 (1998).